Received Date : 19-Oct-2017

Revised Date : 26-Jun-2018

Accepted Date : 10-Aug-2018



# Modification of erythropoietin structure by *N*-homocysteinylation affects its antiapoptotic and proliferative functions

Schiappacasse Agustina, Maltaneri Romina Eugenia, Chamorro María Eugenia, Nesse Alcira Beatriz, Wetzler Diana Elena, Vittori Daniela Cecilia*

Universidad de Buenos Aires. Consejo Nacional de Investigaciones Científicas y Técnicas. Instituto del Departamento de Química Biológica de la Facultad de Ciencias Exactas y Naturales (IQUIBICEN). Departamento de Química Biológica, Facultad de Ciencias Exactas y Naturales. Buenos Aires, Argentina

*Corresponding author:

Daniela Vittori, PhD

Departamento de Química Biológica

Facultad de Ciencias Exactas y Naturales

Universidad de Buenos Aires

Pabellón II, Piso 4, Ciudad Universitaria

Ciudad Autónoma de Buenos Aires, C1428EHA

República Argentina.

TE/FAX: 54-011-4576-3342

E-mail address: dvittori@qb.fcen.uba.ar

Running title

Altered function of homocysteinylated erythropoietin

This article has been accepted for publication and undergone full peer review but has not been through the copyediting, typesetting, pagination and proofreading process, which may lead to differences between this version and the Version of Record. Please cite this article as doi: 10.1111/febs.14632

Article type : Original Articles

Abbreviations

ANS, 8-Anilino-1-naphthalenesulfonic acid; DTT, dithiothreitol; EPO, erythropoietin; FBS, Fetal bovine serum; Hcy, homocysteine; HTL, homocysteine thiolactone; MTT, (3,4,5-dimethylthiazol-2-yl)-2,5-diphenyltetrazolium bromide; PBS, phosphate buffered saline; ThT, thioflavin T.

Keywords

Erythropoietin – *N*-homocysteinylation – Hyperhomocysteinemia – Erythropoietin resistance – Protein Structure

Abstract

Many patients under therapy with recombinant human erythropoietin (rhuEPO) show resistance to the treatment, an effect likely associated with the accumulation of tissue factors, especially in renal and cardiovascular diseases. Hyperhomocysteinemia due to high serum levels of homocysteine has been suggested among the risk factors in those pathologies. Its main effect is the *N*-homocysteinylation of proteins due to the interaction between the highly reactive homocysteine thiolactone (HTL) and lysine residues. The aim of this study was to evaluate the effect of *N*-homocysteinylation on the erythropoietic and antiapoptotic abilities of EPO, which can be a consequence of structural changes in the modified protein. We found that both cellular functions were altered in the presence of HTL-EPO. A decreased net positive charge of HTL-EPO was detected by capillary zone electrophoresis, while analysis of polyacrylamide gel electropherograms suggested formation of aggregates. Far-UV spectra, obtained by Circular Dichroism Spectroscopy, indicated a switch of the protein's secondary structure from $\alpha$-helix to $\beta$-sheet structures. Results of Congo red and Thioflavin T assays confirm the formation of repetitive β-sheet structures, which may account for aggregates. Accordingly, Dynamic Light Scattering analysis showed a markedly larger radius of the HTL-EPO structures, supporting the formation of soluble oligomers. These structural changes might interfere with the conformational adaptations necessary for efficient ligand-receptor interaction, thus affecting the proliferative and antiapoptotic functions of EPO.

The present findings may contribute to explain the resistance exhibited by patients with cardio-renal syndrome to treatment with rhuEPO, as a consequence of structural modifications due to protein *N*-homocysteinylation.

## Introduction

Erythropoietin (EPO) is the main hormone involved in the regulation and maintenance of a physiological number of erythrocytes. Therefore, therapy with recombinant human erythropoietin (rhuEPO) has been successfully used to treat the anemia associated with different pathologies. However, a significant number of patients have been reported to exhibit a deficient response. The uremic syndrome is likely one of the conditions leading to EPO resistance, and the administration of high doses of EPO to this specific population is associated with an increased risk of morbidity and mortality [1-3]. Tissue factors that accumulate in several pathological situations ─most of which were identified as uremic toxins─ have been linked to EPO resistance [4].

Hyperhomocysteinemia is defined by the presence of high serum levels of homocysteine (Hcy), a sulfur-containing, non proteinogenic amino acid biosynthesized from methionine. This condition has been associated with an increased cardiovascular risk in the general population [5]. The major cause of high Hcy levels in chronic renal disease is the impairment of its metabolism by the kidney [6,7]. In patients on hemodialysis ─the main candidates to receive rhuEPO treatment─ the presence of hyperhomocysteinemia has been linked to a negative prognosis [8].

Different mechanisms have been proposed to explain the toxicity of Hcy in uremia [9]. Among them, a potential mechanism has been attributed to the alteration of protein structure by homocysteinylation [10,11]. While Hcy reacts with proteins causing *S*-homocysteinylation of cysteine residues, the highly reactive Hcy derivative, named homocysteine thiolactone (HTL), reacts with the ε-amino groups of lysine residues producing *N*-homocyteinylated proteins (Fig. 1) [10,12]. When plasma proteins are incubated in the presence of HTL, homocysteinylation occurs under physiological conditions and this may lead to protein damage [10].

The functionality of proteins depends on their structural integrity. Several kinds of insults such as oxidative stress, ionizing radiation or drug exposure, as well as the pathophysiological accumulation of reactive metabolites in the body, can induce non-enzymatic post-translational modifications in proteins, thus causing the alteration of their functional properties and denaturation. Besides, it has been reported that *N*-homocysteinylation may cause protein aggregation, as documented for several proteins [10,13-18]. Although different hypothesis have been proposed to describe the pathological consequences of hyperhomocysteinemia in humans, the molecular mechanisms of protein dysfunction are yet poorly understood.

The presence of 8 lysine residues in the primary structure of EPO makes it a potential target for *N*-homocysteinylation, particularly under severe hyperhomocysteinemia, when the levels of circulating homocysteine are markedly increased. Our hypothesis is that HTL may react

with EPO inducing functional alterations in the protein, and consequently leading to EPO therapy resistance. Therefore, this study was conducted to evaluate the possible effects of structural changes derived from the *N*-homocysteinylation of EPO on the biological activity of this protein in erythroid cells. We show that incubation of EPO with HTL not only impairs the antiapoptotic and erythropoietic functions of the protein, but concurrently brings about structural changes in the molecule, which are consistent with the formation of soluble oligomers.

## Results

### *N*-homocysteinylation of recombinant human erythropoietin

It has been reported that HTL specifically reacts with lysine residues in the polypeptide chain and hence lysine-rich proteins are the potential major target of HTL. This covalent modification involves the formation of one homocystamide and the consequent addition of one thiol group to the protein, for each lysine residue reacting with HTL [12]. EPO was incubated with HTL in the following molar ratios: EPO:HTL 1:100 ($HTL_{100}$EPO), 1:1000 ($HTL_{1000}$EPO) and 1:2000 ($HTL_{2000}$EPO). As a first approach to detect the reaction of HTL with EPO, the Ellman's assay was performed to quantify free sulfhydryl groups. $HTL_{100}$EPO showed no significant difference with respect to the control EPO —incubated for the same period in the absence of HTL—, while the amount of free sulfhydryl groups in $HTL_{1000}$EPO and $HTL_{2000}$EPO was ten times higher than in the native protein (Fig. 2).

### Functional alterations of erythropoietin due to *N*-homocysteinylation

In previous works, we demonstrated that the modification of EPO by carbamylation alters its erythropoietic action [19,20]. To evaluate the effect of protein *N*-homocysteinylation on the ability of rhuEPO to stimulate erythroid cell growth and survival, UT-7 cells were cultured in the presence of HTL-EPO samples.

The UT-7 cell line, dependent on EPO to survive, failed to proliferate in 48 h-cultures in the presence of $HTL_{1000}$EPO or $HTL_{2000}$EPO. In contrast, $HTL_{100}$EPO produced a similar effect to that of the native protein (Fig. 3A). Accordingly, only $HTL_{100}$EPO was comparable to control EPO when cell viability was analyzed (Fig. 3B). As shown in Fig. 3C, the metabolic activity of cells treated with $HTL_{1000}$EPO and $HTL_{2000}$EPO was as low as that observed in cells cultured in the absence of the growth factor, and significantly lower than in cultures with EPO or $HTL_{100}$EPO. Furthermore, the decrease in MTT signal as well as in the rate of cell proliferation appears to depend on the degree of modification sustained by EPO, as analyzed by the Ellman's reaction.

To determine whether *N*-homocysteinylation also affects protection of UT-7 cells by EPO, apoptosis was evaluated by fluorescent nuclear staining and phosphatidylserine translocation in cells cultured either without EPO or in the presence of control EPO and HTL-

EPO samples (Fig. 3D-F). In line with the results of UT-7 cell proliferation, Fig. 3 shows an alteration of the antiapoptotic capacity of EPO when the molecule is modified by high concentrations of HTL.

It is worth mentioning that control EPO, which was incubated in the absence of HTL for the same period and conditions as the HTL-treated samples, suffered no alterations in its ability to preserve cell viability, stimulate growth and prevent apoptosis.

Effect of *N*-homocysteinylation on erythropoietin structure

*Electrophoretic mobility*

Since distinct functional abilities were detected between control EPO and the HTL-EPO samples, the following aim was to study if changes in the structure of EPO could explain the inhibition of its functions.

In Capillary Zone Electrophoresis (CZE), *N*-homocysteinylation caused a delay in the migration time of EPO depending on the HTL concentration used (Fig. 4A). This was an expected finding, since the loss of positive charge due to *N*-homocysteinylation of lysine residues predicts a lower mobility in the system used.

The isoelectric points of control EPO and $HTL_{1000}$EPO were calculated by Capillary Isoelectrofocusing (CIEF), obtaining five peaks in the 4.25-5.11 pH range for control EPO and seven peaks with pIs between 4.32-5.15 for $HTL_{1000}$EPO (Fig. 4B). Since rhuEPO is a heterogeneous mixture of isoforms, no single pI is available; therefore, changes in the pIs of each isoform after reaction with HTL cannot be identified by this analysis. A differential interaction of HTL with each EPO isoform may be expected as the amino acid residues are exposed to different carbohydrate environments.

Control and treated EPO samples were also analyzed by native PAGE electrophoresis followed by silver staining (Fig. 5A). The electropherograms revealed several bands in the treated samples which exhibited markedly lower migration rates than the native EPO. These bands may account for modified proteins with different charge/mass ratios. Immunodetection allowed to identify such bands as EPO, as all the bands appearing on the gel (Fig. 5A) were positive for reaction with the anti-EPO antibody (Fig. 5B). These results suggest that treatment of EPO with a high HTL concentration gives rise to larger protein structures. In CZE, total protein charge has a high influence on molecule mobility, contrary to what happens in gel electrophoresis, where this parameter is affected by the charge/mass ratio and by the molecular sieving property of the gel.

In order to explain the different results obtained with both techniques, we analyzed possible structural modifications on HTL-treated EPO.

*Circular Dichroism Spectroscopy (CD)*

Far-UV CD spectroscopy was used to explore the secondary structure of EPO after treatment with HTL. In the Far-UV CD spectra obtained in the 200-260 nm range, native EPO exhibited the typical spectrum of an α-helical protein with the characteristic minima at 208 and 222 nm (Fig. 6A), in agreement with previously reported results for other commercial erythropoietins [21]. As shown in the figure, no significant changes were observed at a low HTL concentration ($HTL_{100}$EPO), whereas in the presence of higher concentrations of HTL, EPO exhibited significant structural transitions, resulting in a pronounced alteration in its relative structural proportions (Fig. 6A, inset). $HTL_{1000}$EPO and $HTL_{2000}$EPO showed a negative CD signal with the contribution of a minimum at 216 nm, typical of a β-sheet conformation. These spectral changes may be due to the conversion of α-helix to repetitive β-sheet. Moreover, CD spectra deconvolution displayed a decrease in α-helical content from 53% in EPO to 28% in $HTL_{2000}$EPO with the concomitant increase in β-sheet conformation from 5% to 18% (Fig. 6A, inset).

Near-UV CD spectroscopy was employed to analyze modifications in the tertiary structure of the protein after HTL treatment. While the aromatic CD signal of $HTL_{100}$EPO was only slightly modified, $HTL_{1000}$EPO and $HTL_{2000}$EPO exhibited a pronounced change in spectral shape (Fig. 6B).

*Intrinsic Fluorescence*

Intrinsic fluorescence spectra were recorded to study the environment of the three tryptophans in the EPO molecule. For this purpose, samples of native and HTL-modified EPO were analyzed at the same final concentration. No differences were observed in the maximum fluorescence wavelength of Trp among the different erythropoietin samples analyzed. Nevertheless, the intensities observed for $HTL_{1000}$EPO and $HTL_{2000}$EPO were higher than those of EPO and $HTL_{100}$EPO (Fig. 7A). This indicates a lower quenching of Trp fluorescence due to modifications in the environment of these residues in the different HTL-EPO preparations. This result suggests that as a consequence of *N*-homocysteinylation, tryptophans are more protected from quenchers, and confirms a change in the tertiary structure of the modified proteins.

*ANS Assays*

As an additional assay, we used spectrofluorometry to examine the binding of ANS to hydrophobic clusters on the protein's surface. Binding of ANS to EPO was confirmed by the characteristic blue shift and the increase in ANS fluorescence emission (Fig. 7B). $HTL_{1000}$EPO and $HTL_{2000}$EPO exhibited a pronounced blue shift and a substantially

increased ANS fluorescence intensity, indicative of the existence of hydrophobic surface areas exposed to the solvent when the repetitive β-sheet structure was formed.

*Congo red and Thioflavin T Assays*

For a better evaluation of the increase in β-sheet structures observed by CD after HTL treatment, the ability of samples to bind Congo red and Thioflavin T (ThT), two dyes usually used to monitor the formation of amyloid structures, was assayed (Fig. 7C and D). Unlike EPO and $HTL_{100}$EPO, the incubation of $HTL_{1000}$EPO and $HTL_{2000}$EPO with the Congo red dye showed a spectral shift to higher wavelengths, which supports the formation of repetitive β-sheet structures previously observed in CD experiments.

While a slight change in the ThT fluorescence spectrum was observed in the presence of $HTL_{100}$EPO, a pronounced increase was detected when EPO was incubated with higher concentrations of HTL. This result confirms the formation of repetitive β-sheet structures in the $HTL_{1000}$EPO and $HTL_{2000}$EPO samples that may account for amyloid fibril precursors [13,22].

*Dynamic Light Scattering (DLS)*

In order to confirm the presence of larger particles in samples of HTL-treated EPO, a DLS analysis was performed. The mean data of radius distribution corresponding to the control and the modified EPO molecules is shown in Fig. 8. While $HTL_{100}$EPO presented a similar size than EPO, markedly larger radii were obtained for the modified proteins $HTL_{1000}$EPO and $HTL_{2000}$EPO, supporting the hypothesis of soluble oligomer formation. The values observed for mean radius suggest the presence of soluble oligomers rather than β-amyloid fibrils. It is worth mentioning that the radius obtained for native EPO is in agreement with data reported in the literature [21].

## Discussion

High serum levels of homocysteine (Hcy) have been found associated with an increased incidence of cardiovascular diseases ─including atherosclerosis [23] and thrombosis [24]─, with chronic kidney disease [6, 25] and with various neurodegenerative pathologies such as dementia and Parkinson's [26] and Alzheimer's [27] diseases.

Methionyl-tRNA synthetase (MetRS) catalyzes the conversion of Hcy to a cyclic and highly reactive thioester (homocysteine thiolactone) which easily acylates free amino groups of protein lysine residues in a process referred to as protein *N*-homocysteinylation [12]. In this context, *N*-homocysteinylated plasma proteins were found significantly increased in end stage renal disease (ESRD) patients with hyperhomocysteinemia [28].

It has been reported that the reaction of HTL with proteins results in the loss of their functions due to alterations in the molecular structure and to a higher sensitivity to oxidative damage [11]. This issue is specially important, since it has been described that in ESRD the prevalence of hyperhomocysteinemia is 85–100% [25].

Erythropoietin is the main growth factor associated with the regulation of red blood cell production. Since expression of the EPO receptor and responsiveness to EPO were observed in non-hematopoietic tissues, this protein is also considered a survival factor for different non-erythroid cells [29,30].

Taking the above mentioned into account, the aim of this work was to evaluate whether EPO could be a target for HTL, and if the functionality of the protein could be affected by *N*-homocysteinylation.

We found that EPO incubated with high concentrations of HTL (EPO:HTL at molar ratios 1:1000 and 1:2000) not only failed to induce proliferation of the EPO-dependent UT-7 cell line, but was also unable to protect these cells from apoptosis (Fig. 3). These results indicate a loss of activity of the modified EPO, in agreement with reports showing that *N*-homocysteinylation is associated with structural and functional alterations of different proteins [11,17,31].

We then went forward to analyze possible structural changes in the EPO molecule due to reaction with HTL, which could explain the detected loss of function.

First, we compared the electrophoretic mobility of the modified proteins with respect to the unmodified EPO by Capillary Zone Electrophoresis (Fig. 4). The electropherograms showed a lower electrophoretic mobility for the modified proteins with an impaired biological function. This was an expected result, as the *N*-homocysteinylation of lysine residues accounts for a decrease in the positive net charge of the protein, despite the fact that a new amino group is added during the reaction. An explanation for the lower positive net charge observed in *N*-homocysteinylated proteins was given by Jakubowski [10], who reported that the ε-amino group of lysine (pK=10.5) is much more basic than the α-amino group of Hcy bound to lysine, (εN(Hcy) lysine, pK=7.1).

However, contrary to what was expected, the separation pattern of the modified proteins analyzed by polyacrylamide gel electrophoresis under native conditions showed bands of HTL-EPO with low electrophoretic mobility (Fig. 5A and 5B). One possible explanation for this phenomenon is the aggregation of the protein induced by *N*-homocysteinylation. In line with these results, many acidic proteins have been reported to form oligomers and aggregates upon modification by HTL [10,13,15,17], which may account for their lack of function.

In order to evaluate possible modifications in the structure of EPO, intrinsic protein fluorescence emission spectra were used to analyze changes in the aromatic amino acid environment. As the concentration of HTL reacting with the protein increased, we observed a higher intensity of fluorescence without change in the emission maxima, confirming that EPO undergoes a structural modification (Fig. 7A). This particular behavior could be attributed to minor polarity changes in the surroundings of tryptophan residues and to the relocation of the tryptophan away from other residues that could act as fluorescence quenchers. It has been reported that residues W51 and W64 are buried within the core of the protein, while W88 appears to be partially exposed to the solvent [32]. Our results suggest that W88 is protected from the quencher as a consequence of the structural changes sustained by the modified EPO.

To further assess the effect of HTL on the EPO molecule, CD spectra were analyzed, revealing significant alterations in the secondary structure of the protein (Fig. 6A). As a member of the hematopoietic growth factor family, the topology of EPO predominantly consists of a left-handed bundle of four α-helices [33], which was transformed into a β-sheet-rich structure after exposure to HTL. Further gaining of a critical amount of β-sheets may give rise to the formation of soluble oligomers that could be precursors of fibril aggregates. In line with these results, the conversion of α-helices to β-sheets due to *N*-homocysteinylation, regardless of aggregate formation, has been previously reported for other proteins, such as bovine insulin [15], caseins [16] and α-lactalbumin [17].

To elucidate whether *N*-homocysteinylation could induce the formation of β-sheet repetitive structures, the ability of EPO samples to bind Congo red and ThT was assayed. When EPO was treated with the highest concentrations of HTL, the observed change of the dye absorbance maximum (Fig. 7A) indicates the presence of β-sheet repetitive structures −possibly soluble oligomers─ that could account for amyloid fibril precursors. The results obtained by the ThT assay (Fig. 7B) are consistent with those of Congo red assay. The ANS binding capacity assay (Fig. 7B) indicated that buried hydrophobic surfaces become accessible to the solvent, an effect that was previously reported for β-sheet soluble oligomers comprised of other proteins [22], and for homocysteinylated proteins [17]. The formation of these soluble oligomers is compatible with the higher mean of radial distribution obtained by DLS for the HTL-treated erythropoietin samples (Fig. 8). This result supports the presence of large structures with low electrophoretic mobility in the gel electrophoresis assays presented in Figure 5.

Alterations in the non-covalent interactions that maintain the structure of a protein may lead to its misfolding or unfolding. This may in turn induce interactions between exposed hydrophobic zones of neighbouring proteins, leading to either amorphous or more structured aggregates like amyloid fibrils. The results from Paoli *et al* [13] reveal that even a low level of *N*-homocysteinylation induced mild conformational changes in bovine serum albumin (BSA). In the presence of HTL, the structure of BSA was converted into a partially unfolded intermediate with a high tendency to form aggregates which undergo a long-term structural

reorganization, leading to the formation of amyloid-like fibrils. There are many examples of peptides or folded proteins, of which some are associated with pathologies, where the soluble oligomers may accumulate or act as fibril precursors [22,34-39]. Based on this knowledge, the loss of biological function observed in EPO after modification with HTL could be explained by misfolding of the protein. This results in the exposure of hydrophobic zones which would ultimately allow the formation of soluble oligomers. An updated review [40] discusses the formation of toxic multimers, aggregates or amyloids resulting from incorporation of HTL into proteins. In this context, this reaction has been suggested as an independent risk factor for different pathologies, particularly neurodegenerative diseases [13,41,42]

In this work, we report for the first time that *N*-homocysteinylation destabilizes the structure of the growth factor erythropoietin, causing the conversion of its α-helices to β-sheet repetitive structures with a high tendency to form soluble oligomers. Based on these results, we suggest that the structural changes in the molecule impair the spatial adaptation required for an efficient ligand-receptor interaction, thus affecting the proliferative and antiapoptotic functions of EPO.

Although further investigation is required, the present findings may contribute to explain the resistance of patients with cardiovascular and renal diseases to EPO treatment, which is frequently associated with hyperhomocysteinemia and consequently, with protein *N*-homocysteinylation.

## Materials and Methods

### Materials

All chemicals were of analytical grade. Iscove's Modified Dulbecco's Medium and the penicillin–streptomycin antibiotic mixture were obtained from Gibco BRL. 3-(4,5-Dimethyl-2-thiazolyl)-2,5-diphenyl-2H-tetrazolium bromide (MTT), 5,5´-dithiobis(2-nitrobenzoic acid) (Ellman's Reagent), Hoechst 33258 dye, L-Homocysteine thiolactone hydrochloride, 25% glutaraldehyde solution, dithiothreitol (DTT) solution, Congo Red dye, 8-Anilino-1-naphthalenesulfonic acid (ANS), Trypan Blue Solution (0.4%) and horseradish peroxidase-conjugated anti-Mouse IgG (A4416) were obtained from Sigma-Aldrich. The primary antibody against EPO (B4-sc5290) was from Santa Cruz Biotechnologies. The Annexin V-FITC Apoptosis Detection Kit I was from BD Transduction Laboratories. The Carrier Ampholytes pH range 3.0–10.0 were from Pharmalyte GE-Healthcare Bio-Sciences AB. Fetal bovine serum (FBS) was purchased from Natocor (Argentina). Recombinant human erythropoietin (rhEPO) was kindly provided by Zelltek (Argentina).

## Cell cultures

The human UT-7 cell line, that shows growth dependence on EPO, was kindly provided by Dr. Patrick Mayeux (Cochin Hospital, Paris, France). Cells were maintained in Iscove's Modified Dulbecco's Medium supplemented with 10% FBS, 100 U/mL penicillin, 100 µg/mL streptomycin and 1 U/mL EPO. Cell cultures were developed at 37 °C in an atmosphere containing 5% $CO_2$ and 100% humidity [43]. The medium was replaced every 2–3 days. Cell viability and proliferation were routinely evaluated by the Trypan blue exclusion test.

## Protein *N*-homocysteinylation

Recombinant human erythropoietin (specific activity: 125 IU/µg) with Mr of 30243 as determined by MALDI-TOF MS, was incubated (24 h, 37 °C) in the presence of different concentrations of HTL (EPO:HTL molar ratios: 1:100, 1:1000 and 1:2000) in phosphate buffered saline (PBS). After the incubation period, the remaining free HTL was eliminated by ultrafiltration and washing with PBS using an Amicon Ultra-4 centrifugal filter (3 kDa cut-off, Merck Millipore) and final protein concentrations were measured (Nanodrop 2000, Thermo Scientific). EPO samples subjected to a similar incubation process in the absence of HTL were used as controls in all the experiments. Analyses were performed using three independent HTL-EPO batches.

## Protein sulfhydryl estimation

The efficiency of EPO *N*-homocysteinylation was monitored by detecting the increase in protein sulfhydryl groups. The Ellman's reaction was applied to detect free sulfhydryl groups in HTL-EPO and control samples using the Ellman's Reagent. According to the manufacturer's instructions, 250 µL of each sample were added to 50 µL of Ellman's Reagent Solution and 2.5 mL of Reaction Buffer and incubated at room temperature for 15 min. Absorbance was measured at 412 nm. The amount of 2-nitro-5-thiobenzoic acid released was estimated from the molar extinction coefficient (ε) of 14,150 $M^{-1}$ $cm^{-1}$, and the results were expressed as µmoles of free sulfydryl per µmol of protein.

## MTT assay

The MTT dye reduction assay, which measures metabolic activity thus reflecting cell viability, was performed as previously described [44]. Cell cultures were developed in 35 mm Petri dishes at a density of $2x10^5$ cells/mL. The medium was removed and cells were incubated with MTT at 0.5 mg/mL final concentration (2 h, 37 °C). After centrifugation (10 min, 9500 xg), the supernatant was removed and the pellet washed with PBS. Finally, 0.04 M HCl in isopropanol (100 µL) was added to dissolve the blue formazan product (reduced MTT), which was quantified by measuring absorbance at 570 nm (with reference to 660 nm) in a microplate reader (BioRad).

Fluorescent nuclear staining of apoptotic cells

Cells (2 x$10^5$ cells/mL) were cultured on slide covers placed in 35 mm Petri dishes. After fixation with Carnoy's solution (methanol:acetic acid, 3:1 v/v) for 10 min at room temperature, the samples were dried at 20 °C, and later exposed to 0.05 g/L Hoechst 33258 dye in PBS for 10 min at room temperature, washed three times with 18 MΩ water and finally mounted with 50% (v/v) glycerol in PBS. Fluorescent nuclei with apoptotic characteristics were detected by fluorescence microscopy at 365 nm (UV) (Zeiss Axiovert 135). Images were acquired using a Nikon Coolpix 5000 camera and digitalized with the AxioVision Software. Differential counting of nuclei was performed by analyzing at least 500 cells [44].

Apoptosis detection by Flow Cytometry

Annexin V and propidium iodide (PI) analysis allows the detection of different stages of apoptosis. The assay was performed according to the instructions of the commercial kit. Briefly, cells were washed twice with cold PBS and then suspended (1x$10^6$/mL) in binding buffer (0.01 M Hepes/NaOH pH 7.4, 0.14 M NaCl, 2.5 mM $CaCl_2$). Annexin V-FITC (5 µL) and PI (5 µL) were added to 100 µL of cell suspension, which was incubated for 15 min at 25 °C in the dark. After addition of 400 µL of binding buffer, events were acquired in a flow cytometer equipped with a 488 nm argon laser (FACSAria II, Becton-Dickinson). The Cyflogic v1.2.1 software was used for data analysis.

Capillary Zone Electrophoresis

Sample analysis was performed at pH 9.9 (150 mM sodium borate buffer) at 6.7 KV (current intensity 50 µA) in a P/ACE MDQ Capillary Electrophoresis System (Beckman Coulter), equipped with a Photo Diode Array (PDA) detector. The sample hydrodynamic injection was performed during 2.5 sec at a pressure of 0.4 psi in a fused silica capillary of 40 cm length (effective length 30 cm) and 50 µm internal diameter. Electropherograms showing migration time vs. absorbance at 214 nm were obtained at 25 °C.

Capillary Isoelectric Focusing (CIEF) [45]

EPO solution in 20 mM Tris pH 8.0 buffer was concentrated in an Amicon Ultra-4 centrifugal filter (3 kDa cut-off, Merck Millipore) to replace PBS.

All CIEF separations were performed using a P/ACE MDQ Capillary Electrophoresis System (Beckman Coulter) equipped with a UV detector and a 280 nm filter. The installed Neutral Capillary (Beckman Coulter, 30.2 cm long, 20 cm effective length, 50 µm i.d) was maintained at 20 °C during assays. The sample mix ─with or without EPO─, consisting of a mixture of pH 3-10 Carrier Ampholytes, iminodiacetic acid (200 mM), peptide pI markers and 6M urea-CIEF Gel, was introduced into the capillary by rinsing it for 99 s at 25 psi. Focusing was

carried out at field strength of 25 kV for 6 min in the reverse polarity setting with 200 mM phosphoric acid as anolyte, and 300 mM sodium hydroxide as catholyte. The focused peaks were chemically mobilized across the detection window by replacing the catholyte vial with a 100 mM ammonium hydroxide solution, and then applying a field strength of 30 kV for 30 min in the reverse polarity setting. The focused protein bands were detected by absorbance at 280 nm. Data were collected and analyzed using the 32 Karat™ Software.

Electrophoresis and Western blotting

Electrophoresis under alkaline nondenaturing conditions using Tris-glycine buffer pH 8.3 (25 mM Tris, 192 mM glycine) was run in a Miniprotean III electrophoretic system (BioRad) using 10% polyacrylamide gels. At the end, two procedures were followed, a) silver staining and b) Western blotting.

a) Nitrate silver staining. The gel was treated with 40% methanol-7% acetic acid solution (30 min) and with 5% methanol-7% acetic acid solution (7 min). After removing the solutions, the gel was immersed in 10% glutaraldehyde (30 min, room temperature). This solution was discarded and the gel was washed with various changes of water during an hour. Then, a 5 µg/mL DTT solution was added and after 30 min replaced by the silver nitrate solution (0.1% w/v) for additional 30 min. After removing the silver solution, the developing solution (3% sodium carbonate, 0.019% formaldehyde) was added until the bands appeared. The process was stopped by addition of 2.3 M sodium citrate.

b) Western blotting. After gel electrophoresis, protein samples were electroblotted onto a nitrocellulose membrane during 1.5 h (transfer buffer: 25 mM Tris, 195 mM glycine, 0.05% SDS, pH 8.3, and 20%, v/v, methanol). Membranes were blocked by 1 h incubation in Tris Buffered Saline (TBS: 25 mM Tris, 137 mM NaCl, 3 mM KCl, pH 7.4) containing 0.1% Tween 20 and 0.5% skim-milk powder [40], and then incubated with appropriate concentrations of anti EPO antibody. After washing with TBS–0.1% Tween 20, the immunoblots were probed with adequate peroxidase-conjugated secondary antibody (1:1000) for 1 h at 20 °C and washed. Antigen-antibody complex signals were detected by enhanced chemiluminiscence in a G:BOX Chemi system and digitalized using the GeneSys software (Syngene).

Circular dichroism (CD)

In order to assess the effect of HTL treatment on the secondary and tertiary structure of EPO, CD measurements were carried out on a Jasco J-815 spectropolarimeter. CD spectra in the far-UV and near-UV region were collected using a Peltier temperature-controlled sample holder at 25 °C in a 0.1-cm path length cell in 25 mM buffer solution. Each spectrum was repeated at least four times. Mean Residual Ellipticity ($[\theta]_{MRW}$ (deg $cm^2dmol^{-1}res^{-1}$) was calculated from measured ellipticity as :

$$[\theta]_{MRW} = \frac{\theta}{C.l.10.N}$$

Where θ is ellipticity in millidegrees, l is the cuvette pathlength in cm, N is the number of residues and C is the molar concentration.

We employed the K2D3 algorithm (http:://k2d3.ogic.ca/) to deconvolute far-UV CD spectrum in order to obtain experimental secondary structure contributions.

Congo red binding assay

A 5 µM final protein concentration of each EPO sample was diluted in PBS containing 2 µM Congo red (CR). Absorption spectra were acquired between 450–650 nm using a UV/Visible spectrophotometer (JascoV650) at 25 °C, with a 10-mm-pathlength cuvette. The spectrum of the protein aliquot in PBS buffer was subtracted from the spectrum of the protein solution in PBS with the addition of CR. The same procedure was followed for each treatment.

Intrinsic, ANS and Thioflavin T fluorescence emission

Fluorescence emission spectra of the samples (10 µM) were obtained in an Aminco-Bowman spectrofluorimeter. Proteins were excited at 295 nm and the emission spectra were recorded in the 310-400 nm wavelength region.

For ANS (8-Anilino-1-naphthalenesulfonic acid) experiments, the excitation wavelength was 350 nm and emission spectra were recorded from 400 to 600 nm using an Aminco-Bowman spectrofluorimeter. Protein concentration was kept at 10 µM and ANS concentration was 100 µM. Blanks were subtracted from each sample. Each spectrum was repeated at least three times.

For ThT experiments, the excitation wavelength was 435 nm and emission spectra were recorded from 460 to 600 nm using an Aminco-Bowman spectrofluorimeter. Protein concentration was kept at 10 µM and ThT concentration was 20 µM.

Dynamic Light Scattering (DLS)

DLS provides information of the speed at which particles diffuse due to Brownian motion. DLS measurements of control and HTL-treated EPO samples were performed in PBS buffer in a Zetasizer Nano S DLS device (Malvern Instruments). Protein concentration was kept at 10 µM in order to prevent possible size modifications derived from the concentration of

samples to higher values. Each sample was measured ten times with ten runs per measurement. The temperature was maintained at 25 °C by a Peltier control system. Results were processed with the software included in the equipment to obtain particle size values.

## Statistics

Statistical analysis was performed with the GraphPad Prism software (GraphPad Software Inc.). Whenever applied, ANOVA and Kruskal-Wallis one-way analysis of variance were followed by Dunnet's or Dunn's test for comparison among groups, respectively. Least significant difference with $P<0.05$ was considered the criterion for statistical significance.

## Acknowledgements

The authors are grateful to Zelltek S.A. (Argentina) for supplying human recombinant erythropoietin and to Lic. Silvana Gionco for her assistance in Capillary Electrophoresis analyses. This work was supported by the Universidad de Buenos Aires (UBACYT 20020130110024 6BA), the Consejo Nacional de Investigaciones Científicas y Técnicas (CONICET 11220150100804CO) and the Agencia Nacional de Promoción Científica y Tecnológica (ANPCYT-PICT 13-0692). Dr. Alcira Nesse, Dr. Daniela Vittori, Dr. Diana Wetzler and Dr. María E. Chamorro are research scientists at the CONICET, and Dr. Romina Maltaneri and Lic. Agustina Schiappacasse have received fellowships from the CONICET (Argentina).

## Authors Contributions

DV conceived and designed the study, carried out analysis of protein structure, and supervised the whole study as well as the manuscript drafting and approval. AS carried out the experimental assays and analysis of the results, and contributed to writing the paper. RM and MEC participated in the performance of laboratory assays and analysis of data. RM revised the English grammar. AN contributed to the study design, participated in drafting the manuscript and performed the critical revision of the final version. DW organized and carried out protein structure assays, participating in the critical discussion of data and final manuscript.

## References

1. Abe M, Okada K, Maruyama T, Matsumoto K & Soma M (2011) Relationship between erythropoietin responsiveness, insulin resistance, and malnutrition inflammation-atherosclerosis (MIA) syndrome in hemodialysis patients with diabetes. Int J Artif Organs 34, 16-25.

2. Garimella P, Katz R, Patel K, Kritchevsky S, Parikh Ch, Ix J, Fried LF, Newman AB, Shlipak MG, Harris TB & Sarnak MJ (2016) Association of serum erythropoietin with

cardiovascular events, kidney function decline, and mortality: The health aging and body composition study. Circ Heart Fail 9:e002124, doi: 10.1161/CIRCHEARTFAILURE.115.002124.

3. Grote Beverborg N, van der Wal H, Klip I, Voors A, de Boer R, van Gilst W, van Veldhuisen DJ, Gansevoort RT, Hillege HL, van der Harst P, Bakker SJ & van der Meer P (2016) High serum erythropoietin levels are related to heart failure development in subjects from the general population with albuminuria: data from PREVEND. Eur J Heart Fail 18, 814-821.

4. Nangaku M, Mimura I, Yamaguchi J, Higashijima Y, Wada T & Tanaka T (2015) Role of uremic toxins in erythropoiesis-stimulating agent resistance in chronic kidney disease and dialysis patients. J Renal Nutr 25, 160-163.

5. Jourde-Chiche N, Dou L, Cerini C, Dignat-George F & Brunet P (2011) Vascular incompetence in dialysis patients. Protein-bound uremic toxins and endothelial dysfunction. Semin Dial 24, 327-337.

6. Friedman AN, Bostom AG, Selhub J, Levey AS & Rosenberg IH (2001) The kidney and homocysteine metabolism. J Am Soc Nephrol 12, 2181-2189.

7. Potter K, Hankey GJ, Green DJ, Eikelboom JW & Arnolda LF (2008) Homocysteine or renal impairment. Which is the real cardiovascular risk factor? Arterioscler Thromb Vasc Biol 28, 1158-1164.

8. Mallamaci F, Bonanno G, Seminara G, Rapisarda F, Fatuzzo P, Candela V, Scudo P, Spoto B, Testa A, Tripepi G, Tech S & Zoccali C (2002) Hyperhomocysteinemia predicts cardiovascular outcomes in hemodialysis patients. Kidney Int 61, 609–614.

9. Perna AF, Ingrosso D, Lombardi C, Acanfora F, Satta E, Cesare CM, Violetti E, Romano MM & De Santo NG (2003) Possible mechanisms of homocysteine toxicity. Kidney Int 84, S137–S140.

10. Jakubowski H (1999) Protein homocysteinylation: possible mechanism underlying pathological consequences of elevated homocysteine levels. FASEB J 13, 2277–2283.

11. Jakubowski H (2004) Molecular basis of homocysteine toxicity in humans. Cell Mol Life Sci 61, 470–487.

12. Jakubowski H (1997) Metabolism of homocysteine thiolactone in human cell cultures. Possible mechanism for pathological consequences of elevated homocysteine levels. J Biol Chem 272, 1935-1942.

13. Paoli P, Sbrana F, Tiribilli B, Caselli A, Pantera B, Cirri P, De Donatis A, Formigli L, Nosi D, Manao G, Camici G & Ramponi G (2010) Protein N-homocysteinylation induces the formation of toxic amyloid-like protofibrils. J Mol Biol 400, 889-907.

14. Glowacki R & Jakubowski H (2004) Cross-talk between Cys34 and Lysine Residues in human serum albumin revealed by *N*-Homocysteinylation. J Biol Chem 279, 10864–10871.

15. Jalili S, Yousefi R, Papari M-M & Moosavi-Movahevi A (2011) Effect of homocysteine thiolactone on structure and aggregation propensy of bovine pancreatic insulin. Protein J 30, 299-307.

16. Stroylova Y, Zimny J, Yousefi R, Chobert J-M, Jakubowski H, Muronetz V & Haertlé T (2011) Aggregation and structural changes of αS1-, β- and κ-caseins induced by homocysteinylation. Biochim Biophys Acta 1814, 1234-1245.

17. Sharma GS, Kumar T & Singh LR (2014) N-homocysteinylation induces different structural and functional consequences in acidic and basic proteins. PLoS ONE 9:e116386.

18. Khodadadi S, Riazi GH, Ahmadian S, Hoveizi E, Karima O & Aryapour H (2012) Effect of N-homocysteinylation on physicochemical and cytotoxic properties of amyloid β-peptide. FEBS Letters 586, 127-131.

19. Chamorro ME, Wenker SD, Vota DM, Vittori DC & Nesse AB (2013) Signaling pathways of cell proliferation are involved in the differential effect of erythropoietin and its carbamylated derivative. Biochim Biophys Acta 1833, 1960–1968.

20. Chamorro ME, Maltaneri RE, Vittori DC & Nesse AB (2015) Protein tyrosine phosphatase 1B (PTP1B) is involved in the defective erythropoietic function of carbamylated erythropoietin. Int J Biochem Cell Biol 61, 63–71.

21. Deechongkit S, Aoki KH, Park SS & Kerwin BA (2006) Biophysical comparability of the same protein from different manufacturers: a case study using Epoetin alfa from Epogen and Eprex. J Pharm Sci 95, 1931-1943, doi: 10.1002/jps.20649.

22. Wetzler DE, Castano EM & de Prat-Gay G (2007) A quasi-spontaneous amyloid route in a DNA binding gene regulatory domain: The papillomavirus HPV16 E2 protein. Protein Sci 16, 744–754.

23. Lawrence de Koning AB, Werstuck GH, Zhou J & Austin RC (2003) Hyperhomocysteinemia and its role in the development of atherosclerosis. Clin Biochem 36, 431-441.

24. den Heijer M, Koster T, Blom HJ, Bos GM, Briet E, Reitsma PH, Vandenbroucke JP & Rosendaal FR (1996) Hyperhomocysteinemia as a risk factor for deep-vein thrombosis. N Engl J Med 334, 759-762.

25. van Guldener C (2006) Why is homocysteine elevated in renal failure and what can be expected from homocysteine-lowering? Nephrol Dial Transplant 21, 1161-1166.

26. Doherty GH (2013) Homocysteine and Parkinson's disease: a complex relationship. J Neurol Disord 1:107, doi:10.4172/2329-6895.1000107

27. Morris MS (2003) Homocysteine and Alzheimer's disease. Lancet Neurol 2, 425-428.

28. Perna AF, Satta E, A Canfora F, Lombardi C, Ingrosso D & De Santo NG (2006) Increased plasma protein homocysteinylation in hemodialysis patients. Kidney Int 69, 869-876.

29. Rui T, Feng Q, Lei M, Peng T, Zhang J, Xu M, Abel ED, Xenocostas A & Kvietys PR (2004) Erythropoietin prevents the acute myocardial inflammatory response induced by ischemia/ reperfusion via induction of AP-1. Cardiovasc Res 65, 719-727.

30. Noguchi CT, Asavaritikrai P, Teng R & Jia Y (2007) Role of erythropoietin in the brain. Clin Rev Oncol Hematol 64, 159-171.

31. Sauls DL, Lockhart E, Warren ME, Lenkowski A, Wilhelm SE & Hoffman M (2006) Modification of fibrinogen by homocysteine thiolactone increases resistance to fibrinolysis: a potential mechanism of the thrombotic tendency in hyperhomocysteinemia. Biochemistry 45, 2480-2487.

32. Lah J, Prislan I, Krzan B, Salobir M, Francky A & Vesnaver G (2005) Erythropoietin unfolding: thermodynamics and its correlation with structural features. Biochemistry 44, 13883-13892.

33. Cheetham JC, Smith DM, Aoki, KH, Stevenson JL, Hoeffel TJ, Syed RS, Egrie J & Harvey TS (1998) NMR structure of human erythropoietin and a comparison with its receptor bound conformation. Nat Struct Biol 5, 861-866, doi: 10.1038/2302

34. Chen YR & Glabe CG (2006) Distinct early folding and aggregation properties of Alzheimer amyloid-beta peptide Abeta40 and Abeta42: Stable trimer or tetramer formation by Abeta42. J Biol Chem 34, 24414-24422.

35. Lindgren M, Sorgjerd K & Hammarstrom P (2005) Detection and characterization of aggregates, prefibrillar amyloidogenic oligomers, and protofibrils using fluorescence spectroscopy. Biophys J 88, 4200-4212.

36. Kelly JW (1996) Alternative conformations of amyloidogenic proteins govern their behavior. Curr Opin Struct Biol 6, 11–17.

37. Smal C, Alonso LG, Wetzler D, Heer A & Prat Gay G (2012) Ordered self-assembly mechanism of a spherical oncoprotein oligomer triggered by zinc removal and stabilized by an intrinsically disordered domain. PLoS ONE 7, e36457. doi:10.1371/journal.pone.0036457

38. Ecroyd H & Carver JA (2009) Crystallin proteins and amyloid fibrils. Cell Mol Life Sci 66, 62–81.

39. Bitan G, Kirkitadze MD, Lomakin A, Vollers SS, Benedek GB & Teplow DB (2003) Amyloid beta-protein (Abeta) assembly: Abeta 40 and Abeta 42 oligomerize through distinct pathways. Proc Natl Acad Sci (USA) 100, 330–335.

40. Kumar T, Sharma GS & Singh LR (2016) Homocysteinuria: Therapeutic approach. Clin Chim Acta 458, 55-62.

41. Sengupta U, Nilson AN & Kayed R (2016) The Role of Amyloid-β Oligomers in Toxicity, Propagation, and Immunotherapy. EBioMedicine 6:42-49.

42. Sharma GS, Kumar T, Dar TA & Singh LR (2015) Protein N-homocysteinylation: From cellular toxicity to neurodegeneration. Biochim Biophys Acta 1850, 2239–2245.

43. Vittori D, Pregi N, Pérez G, Garbossa G & Nesse A (2005) The distinct erythropoietin functions that promote cell survival and proliferation are affected by aluminum exposure through mechanisms involving erythropoietin receptor. Biochim Biophys Acta 1743, 29-36.

44. Vittori D, Vota D, Callero M, Chamorro ME & Nesse A (2010) c-FLIP is involved in erythropoietin-mediated protection of erythroid-differentiated cells from TNF-α-induced apoptosis. Cell Biol Int 34, 621-630.

45. Mack S, Cruzado-Park ID & Ratnayake CK. P-12582A Establishing cIEF Separation Conditions for Highly Acidic Proteins. Discovery Products, Beckman Coulter, Inc., Fullerton, CA, https://ls.beckmancoulter.co.jp/files/downloads/PA800plus/P-12582A.pdf

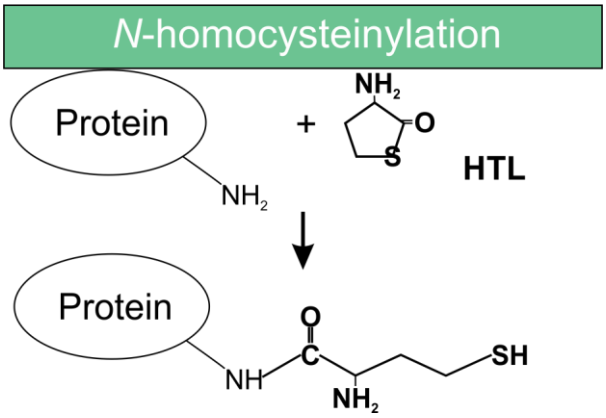


Figure 1. Schematic representation of the reaction between homocysteine thiolactone and the ε-amino group of a lysine residue (Based on the mechanism of acylation of protein lysine residues by HTL, proposed by Jakubowski, 1997, [12]).

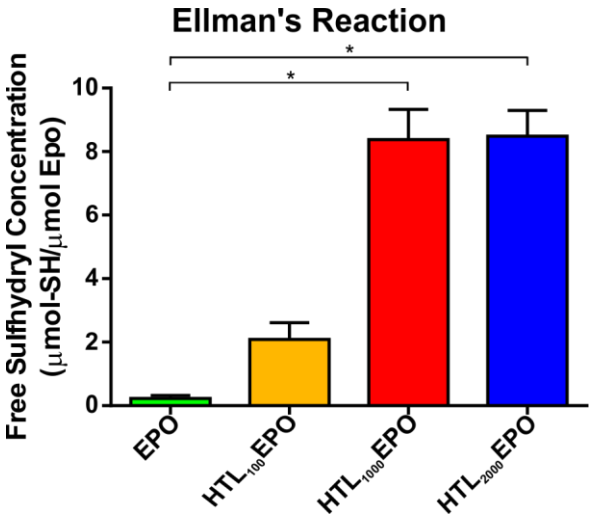


Figure 2. *N*-homocysteinylation efficiency. The Ellman's reagent interacts with free sulfhydryl groups giving a colored reaction. Results are reported as µmoles of free sulfhydryl per µmol of protein. Free sulfhydryl, incorporated into EPO by *N*-homocysteinylation, increase as the concentration of HTL rises (Kruskal-Wallis and Dunn's multiple comparisons test. Significant differences: *P<0.05, Mean ± SEM, n=3).

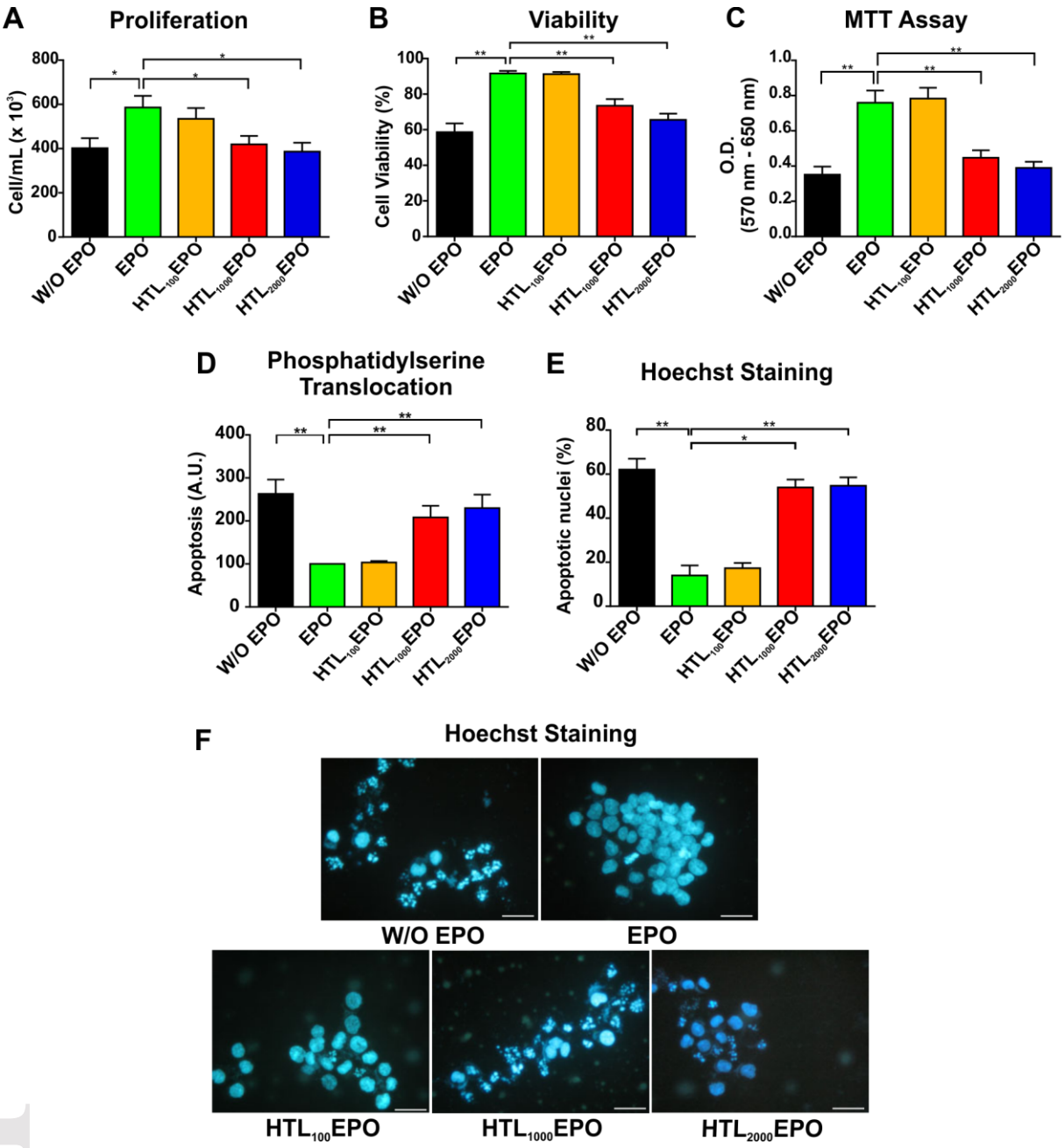


Figure 3. Effect of *N*-homocysteinylation on EPO functions. EPO-dependent UT-7 cells were cultured for 48 h in the presence of HTL-treated or untreated EPO samples (8 ng/mL final concentration). The Trypan Blue Assay was used to evaluate cell proliferation (A) and viability (B). Incubation in the presence of $HTL_{100}EPO$ allowed cells to proliferate at a similar level as that of control EPO, while treatments with $HTL_{1000}EPO$ or $HTL_{2000}EPO$ failed to induce cell proliferation. C) Metabolic activity of UT-7 cells was analyzed by the MTT Assay. The results were in accordance with those of cell proliferation and viability. Statistical analysis by ANOVA followed by Dunnet's multiple comparison test. Significant differences: *P<0.05, **P<0.01, Mean ± SEM, n=8. D) Phosphatidylserine translocation was used to evaluate apoptosis by flow cytometry. Protein *N*-homocysteinylation produced by high HTL concentrations affected the antiapoptotic action of EPO. E-F) Apoptosis was also evaluated by fluorescence microscopy after Hoechst staining (Microphotographs 400 ×, scale bar: 45 µm). A significantly higher number of apoptotic cells was observed in $HTL_{1000}EPO$ or

$HTL_{2000}$EPO-treated cultures compared with those treated with control EPO or $HTL_{100}$EPO (Kruskal-Wallis followed by Dunn's multiple comparisons test. Significant differences: *P<0.05, **P<0.01, Mean ± SEM, n=4).

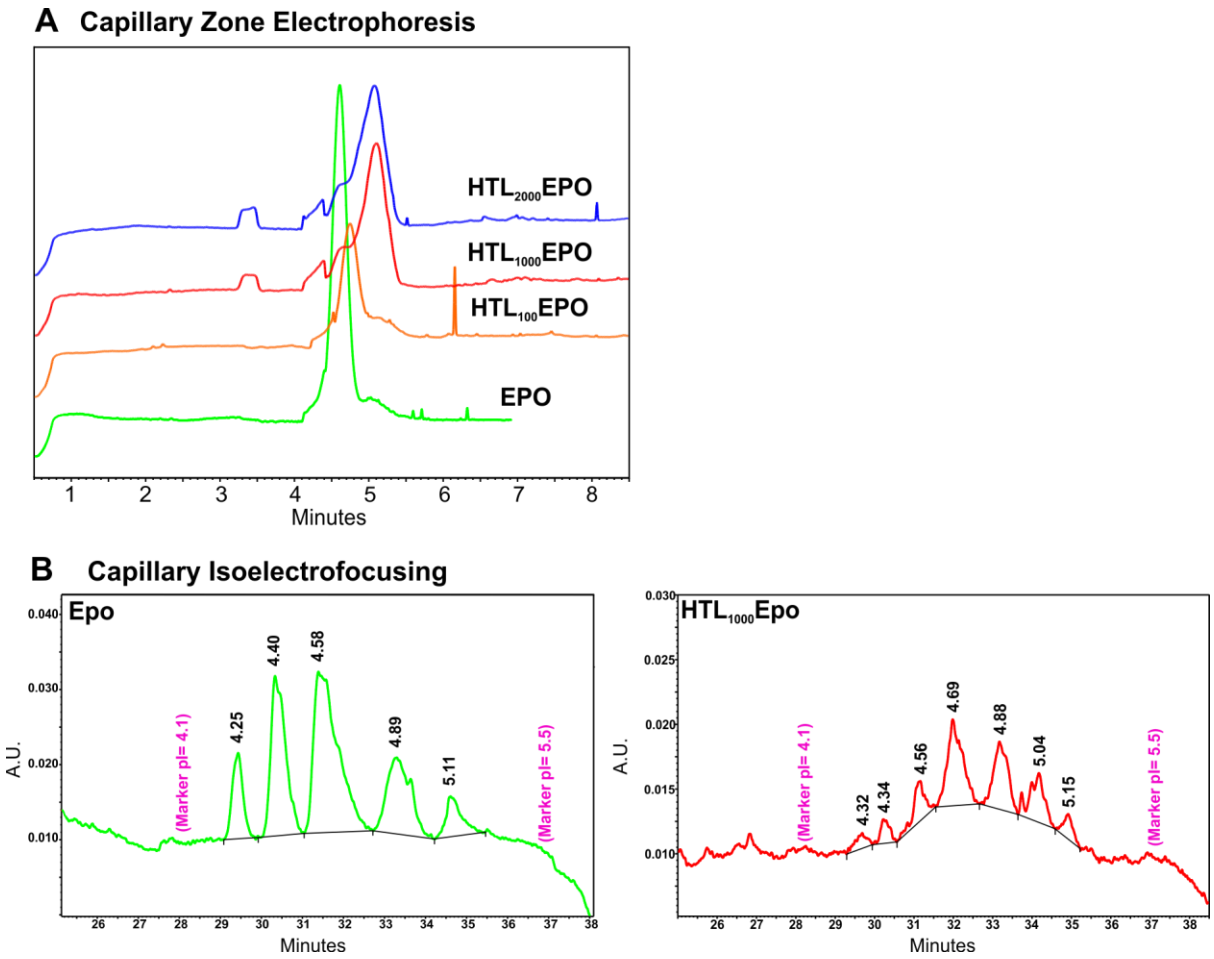


Figure 4. Capillary Electrophoresis. A) CZE was used to evaluate possible changes in the charge/mass ratio of the molecule after *N*-homocysteinylation. As HTL interacts with lysine residues, the net positive charge of EPO diminishes causing a delay in the migration time of HTL-EPO when compared with the unmodified EPO (EPO: 4.17 min, $HTL_{100}$EPO: 4.25 min, $HTL_{1000}$EPO:4.60 min and $HTL_{2000}$EPO: 4.58 min). B) CIEF analysis shows similar pI ranges for both samples studied (control EPO and $HTL_{1000}$EPO).

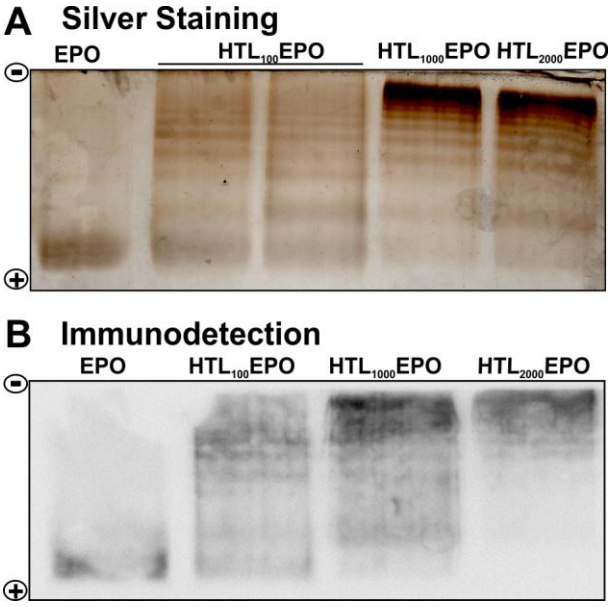


Figure 5. PAGE electrophoretic mobility of EPO. Proteins analyzed by (A) PAGE under native conditions were detected by silver staining (two different samples of $HTL_{100}EPO$ were applied) and (B) Western blotting with an anti-EPO antibody. When treated with high HTL concentrations, the N-homocysteinylated EPO forms larger structures which tend to decrease the rate of protein migration. The gel and immunoblot shown are representative of three independent experiments.

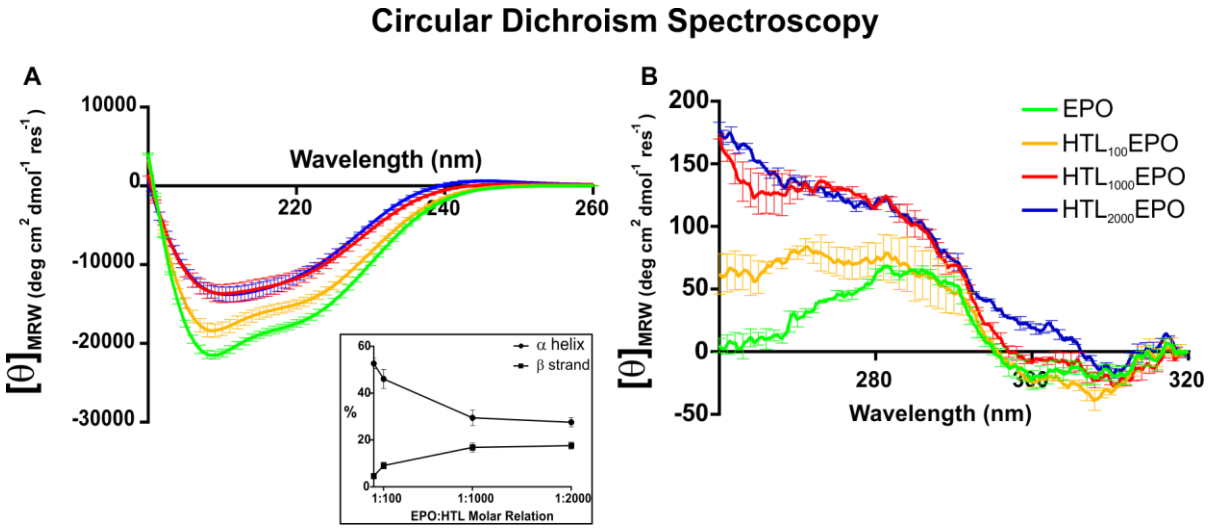


Figure 6. Circular Dichroism spectra of EPO. A) Far-UV Circular Dichroism spectra were used to evaluate the secondary structure of proteins. $HTL_{1000}EPO$ and $HTL_{2000}EPO$ showed a decreased percentage of helical content and a concomitant increase in the percentage of β-sheet structural composition. The percentages of α-helix and β-strand in each sample were plotted with the K2D3 algorithm (inset). B) Near-UV CD spectra were used to analyze changes in the tertiary structure. Results are expressed as Mean ± SEM of 3 independent experiments.

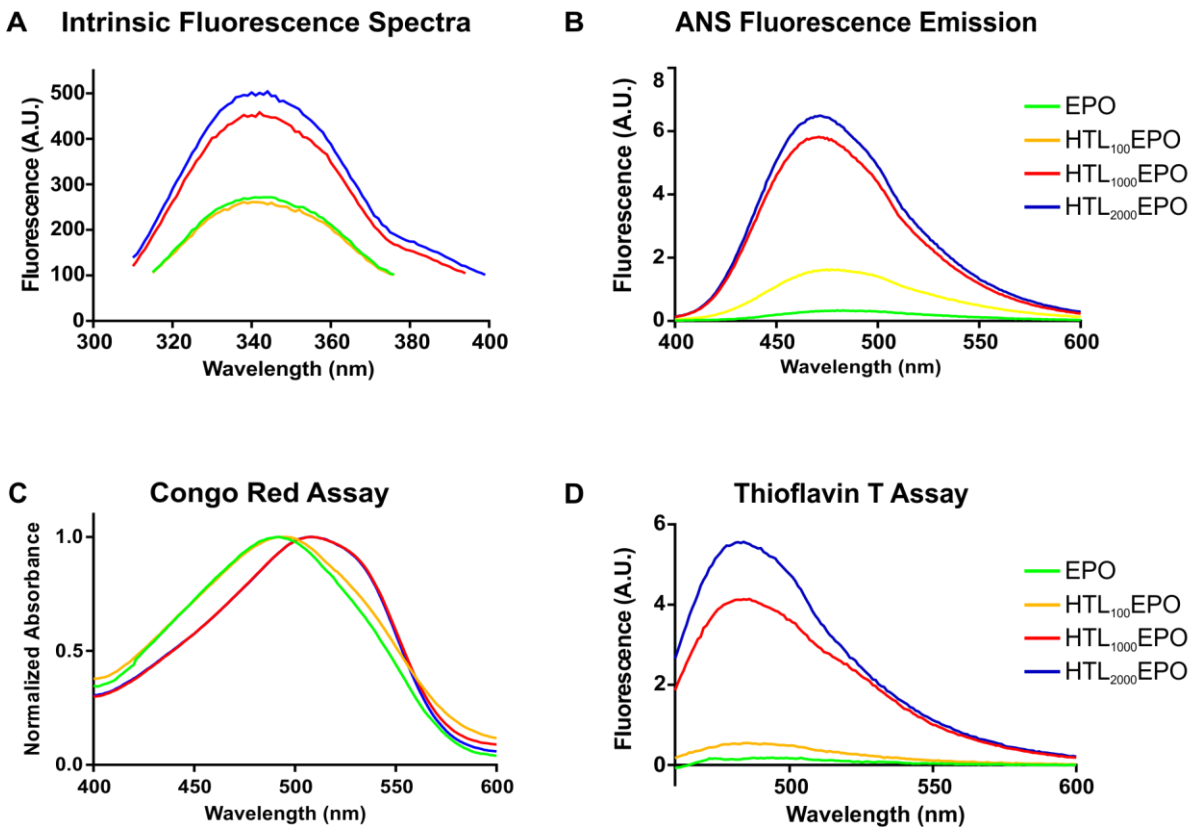


Figure 7. Intrinsic fluorescence spectra, ANS binding, Congo red and Thioflavin T assays. A) Intrinsic fluorescence spectra were obtained to evaluate possible alterations in the local environment of the proteins due to *N*-homocysteinylation. Higher fluorescence intensity was observed for the proteins treated with high HTL concentrations, although no changes in the maximal emission spectrum were detected. B) The appearance of a hydrophobic surface area was analyzed by ANS-binding experiments. A marked increase in ANS binding was detected in the $HTL_{1000}EPO$ and $HTL_{2000}EPO$ samples. C) The Congo red assay showed the presence of repetitive β-sheet structures. Unlike EPO and $HTL_{100}EPO$, $HTL_{1000}EPO$ and $HTL_{2000}EPO$ shifted their maximum absorbance to higher wavelengths. D) The Thioflavin T assay also indicates the presence of repetitive β-sheet structures inthe $HTL_{1000}EPO$ and $HTL_{2000}EPO$ samples by the increase of absorbance and the shift of their maximum absorbance wavelength. Graphs are representative of different experiments.

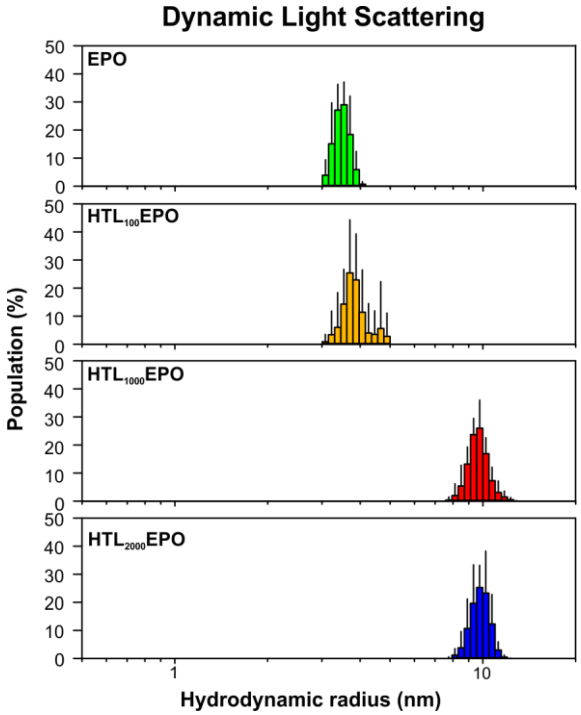


Figure 8. Hydrodynamic radius of HTL-treated EPO. The values represent Mean ± SD of radius distribution corresponding to the control and modified EPO particles. Each sample was measured 10 times with 10 runs/measurement. The values for the different EPO samples were EPO: 3.48±0.14 nm; $HTL_{100}$EPO:3.76±0.46 nm; $HTL_{1000}$EPO: 9.68±0.34 nm; $HTL_{2000}$EPO: 9.80±0.39 nm.